SLAC-PUB-10985
Jan 2005

TiN and TiZrV Thin Film as a Remedy Against Electron Cloud*

F. Le Pimpec, R.E. Kirby, F. King, M. Pivi[1]

Stanford Linear Accelerator Center, Stanford University, Stanford, CA 94309, USA

Abstract

In many accelerators running positively charged beams, ionization of residual gas and secondary electron emission in the beam pipe will give rise to an electron cloud which can cause beam blow-up or the loss of the circulating beam. One solution to avoid the electron cloud is to ensure that the vacuum wall has low secondary emission yield (SEY). The SEY of thin films of TiN and sputter-deposited non-evaporable getter were measured for a variety of conditions, including the effect of recontamination in an ultra high vacuum environment.

Submitted to the journal
Nuclear Instruments and Methods in Physics Research : A

*Work supported by Department of Energy under contracts DE-AC02-76SF00515.

[1]mpivi@slac.stanford.edu.

TiN and TiZrV Thin Film as a Remedy Against Electron Cloud

F. Le Pimpec, R.E Kirby [1], F.King, M.Pivi

SLAC, 2575 Sand Hill Road Menlo Park CA 94025 , USA

Abstract

In many accelerators running positively charged beams, ionization of residual gas and secondary electron emission in the beam pipe will give rise to an electron cloud which can cause beam blow-up or the loss of the circulating beam. One solution to avoid the electron cloud is to ensure that the vacuum wall has low secondary emission yield (SEY). The SEY of thin films of TiN and sputter-deposited non-evaporable getter were measured for a variety of conditions, including the effect of recontamination in an ultra high vacuum environment.

Key words: Thin film, multipacting, getter, NEG, electron cloud, secondary electron emission, secondary electron yield,

1 Introduction

Beam-induced multipacting, which is driven by the electric field of successive positively charged bunches, arises from a resonant motion of electrons that have been initially generated by photons, by gas ionization, or by secondary electron emission (SEE) from the vacuum wall chamber. These electrons move resonantly along the surface of the vacuum chamber, occasionally getting "kicked" by the circulating beam to the opposite wall. The electron "cloud" density depends on characteristics of the positively charged circulating beam (bunch length, charge and spacing) and the secondary electron yield energy spectrum of the wall surface from which the initial electrons are generated. The electron cloud (EC) effect, started by multipacting, has been

[1] E-mail: rek@slac.stanford.edu

[1] DOE contract DE-AC02-76SF00515

observed or is expected at many storage rings [1]. The space charge from the cloud, if sufficiently dense, can lead to a loss of the beam or, at least, to a drastic reduction in beam luminosity.

The SEY of technical surfaces, needed to mitigate multipactor, EC or space charges, has been measured in the past at SLAC [2,3,4], at CERN [5,6,7] and in other labs [8,9,10,11,12]. The term technical surface refers to a mill-finish surface which is commercially available and then chemically cleaned for ultra high vacuum (UHV) use. Technical surfaces have, generally, an SEY higher than the pure material because they are oxidized.

2 Experiment Description and Methodology

The system used to measure SEY, shown schematically in Fig.1 and thoroughly described in [13], is composed of two coupled stainless steel (S/S) UHV chambers where the pressure is in the low 10^{-10} Torr scale in the measurement chamber and high 10^{-9} Torr scale in the load lock chamber. Samples individually screwed to a carrier plate, are loaded first onto an aluminium transfer plate in the load lock chamber, evacuated to a low 10^{-8} Torr scale, and then transferred to the measurement chamber. Pressures are in Torr equivalent N_2.

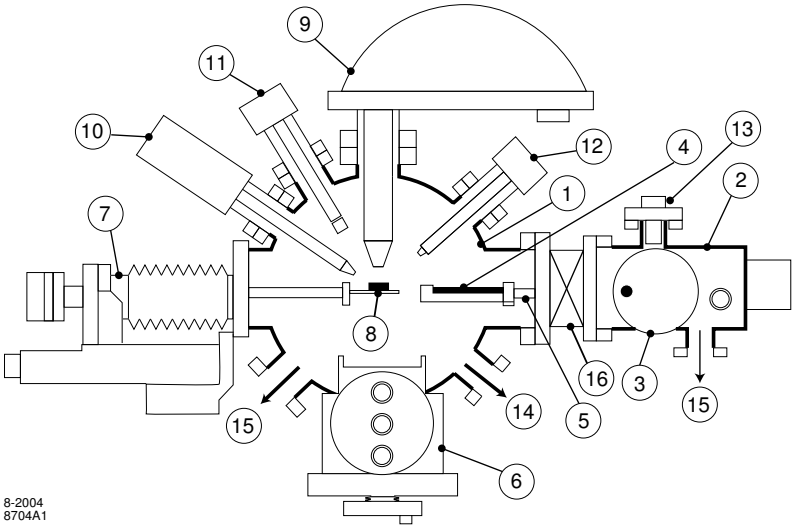

Figure 1. Experimental setup

(1) Analysis chamber
(2) Load lock chamber
(3) Sample plate entry
(4) Sample transfer plate
(5) Rack and pinion travel
(6) Sample plate stage
(7) XYZ θ Omniax^{TM} manipulator
(8) Sample on XYZ θ
(9) Electrostatic energy analyzer
(10) X-ray source
(11) SEY/SEM electron gun
(12) Microfocus ion gun
(13) Sputter ion gun
(14) To pressure gauges and RGA
(15) To vacuum pumps
(16) Gate valve

The measurement chamber has two electron guns and a soft (1.49 keV) x-ray source. One electron gun (energy, 1-3 keV) is used for SEY and SEM, and the other is a "flood" gun for electron conditioning. The x-ray source is used to excite photoelectrons for surface chemical valence and stoichiometry analysis, called ESCA (Electron Spectroscopy for Chemical Analysis), also called XPS (X-ray Photoelectron Spectroscopy). Principles of surface analysis techniques can be found in [14]. The information depth for XPS is < 5 nm, much less than the film thickness of the samples in this study.

After all samples (up to ten or so) are transferred into the measurement chamber, one sample at a time is loaded, on its individual carrier plate, onto an XYZ θ manipulator arm (Vacuum Generators Omniax®). Two thermocouples are available to measure the temperature near the sample, during irradiation or during a sample bake. The back of the samples are heated by electron bombardment, achieved by biasing a tungsten filament negatively with a grounded sample [13].

A good way to monitor the activation process of the TiZrV non-evaporable getter (NEG) is to record the decrease of the surface oxygen concentration with XPS. During the NEG activation, the surface goes from an oxidized state to a partially metallic state. During XPS measurement the x-ray generated photoelectron current leaving the surface of the sample is measured to be $\sim$27 nA, over an area of 16 mm^2. It should be noted that hot Zr is pyrophoric. This is also true for Zr-based alloyed getter like St707^{TM} ($Zr_{70}V_{24.6}Fe_{5.4}$). However, a sample of our $Ti_{27}Zr_{31}V_{42}$ getter, prepared by SAES Getters®, of about 1 micron thickness, did not ignite in air when heated up to 350°C.

The electronic circuit for SEY measurement is presented in Fig.2 [4]. The energy of the computer-controlled electron beam coming from the gun is decoupled from the target measurement circuitry. However, the ground is common to both. The target is attached to a Keithley 6487, a high resolution electrometer with internal variable $\pm$505 V supply and IEEE-488 interface. Filter modes of the K6487 were turned off for our measurements. The integration time for each current reading was 167 μs, which is the minimum value for the instrument. The current was sampled one hundred times; the mean and standard deviation were returned from the K6487 to the computer.

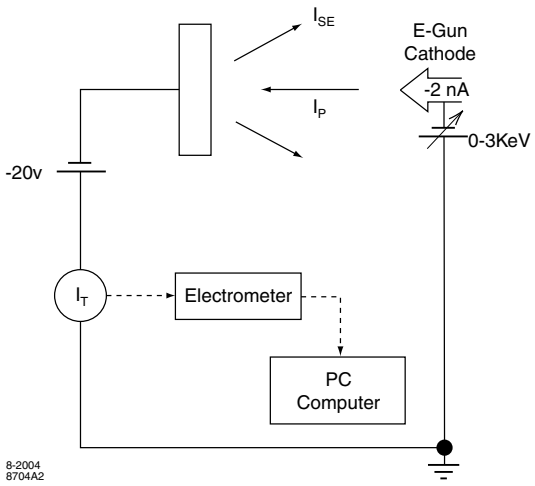

Figure 2. Electronic circuitry used to measure the secondary emission yield

The SEY (δ) definition is determined from equation (1). In practice equation (2) is used because it contains parameters directly measured in the experiment.

$$\delta = \frac{Number\ of\ electrons\ leaving\ the\ surface}{Number\ of\ incident\ electrons} \quad (1) \qquad \delta = 1 - \frac{I_T}{I_P} \quad (2)$$

I_P is the primary current (the current leaving the electron gun and impinging on the surface of the sample) and I_T is the total current measured on the sample ($I_T = I_P + I_{SE}$). I_{SE} is the secondary electron current leaving the target.

The selected 2 nA gun current is measured for a gun energy of 0-100 eV by energy steps of 10 eV (0-3000 eV range) over an area of less than a mm^2. Typically, the beam size is between 0.2 mm to 0.4 mm in diameter. The low current is necessary in order to minimize surface conditioning during SEY measurement. The size of the beam can be checked by using a fluorescent screen, or is inferred from secondary electron microscopical imaging (available on the measurement system and used to precisely choose the point of SEY measurement).

The measurement of the SEY is done while biasing the sample to -20 V. This retarding field repels most secondaries from adjacent parts of the system that are excited by the elastically reflected primary beam. The primary beam current function is measured and recorded each time before an SEY measurement, by biasing the target to +150 V, and with the same step in energy for the electron beam. A fresh current lookup table is created with each measurement. More details on the experimental system and methodology can be found in [13]

The SEY curves were obtained with a beam impinging at 23° from normal incidence or at normal incidence, also labelled "0 deg". The effect on the SEY at such angles of incidence is plotted in Fig.3. A relationship between the SEY for each angle of incidence can be deduced from equation (3), reference [4], and used for comparison with other data.

$$\delta_\theta = \delta_\perp \, e^{\alpha X_m \, (1-\cos(\theta))} \tag{3}$$

Where θ is the angle of incidence of the incoming electron beam, X_m the average depth of escape of the electrons and α the secondary electron absorption. The product $\alpha \, X_m$ can be deduced for TiN and TiZrV from Fig.3

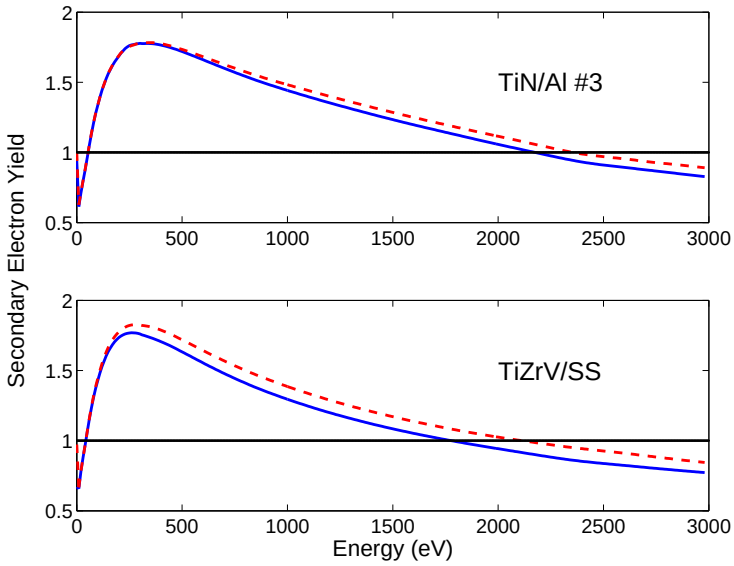

Figure 3. SEY from electrons hitting the same surface, successively, at normal incidence (solid line) and at 23° (dashed line)

3 Results and Comments for TiN thin films

3.1 Variation of the SEY of as received TiN films

TiN coating is commonly used to mitigate multipacting in accelerator and storage ring structures [15]. The TiN coatings measured here were deposited at Brookhaven National Laboratory (BNL) onto 6063 aluminium alloy substrates (TiN/Al) and onto type 304 stainless steel substrate (TiN/SS), using the same procedure and setup described in [9]. The expected film thickness was around 1000 Å. We measured the sample thicknesses using XRF (x-ray fluorescence) [13,14]. The results presented in Fig.4 were obtained by comparing the Ti

x-ray intensities from two reference samples of known thickness: a 157.6 nm thick TiN/Al and a 204 nm thick TiN/SS.

Samples of TiN/Al are referred to by numbers 1-6. Samples of TiN/SS are named by letters a-f.

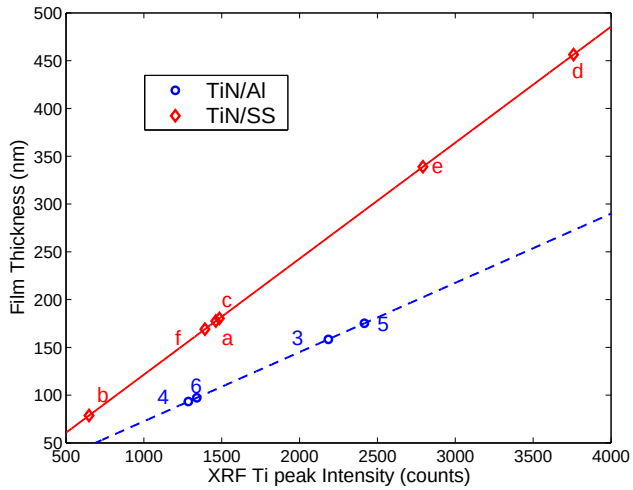

Figure 4. XRF measurements of TiN/Al (X-ray at 7 keV) and TiN/SS (X-ray at 5.5 keV) thin sputter-deposited films, with their respective fits.

The measured δ_{max} of the TiN/Al samples, as shown in Fig.5, varies from 1.5 to 2.5, with the thickest samples displaying the lowest SEY. The variation at the SEY maximum may be due to non-uniform samples emitting secondaries with two different yields. The result would be a superposition of two, or more, SEY curves.

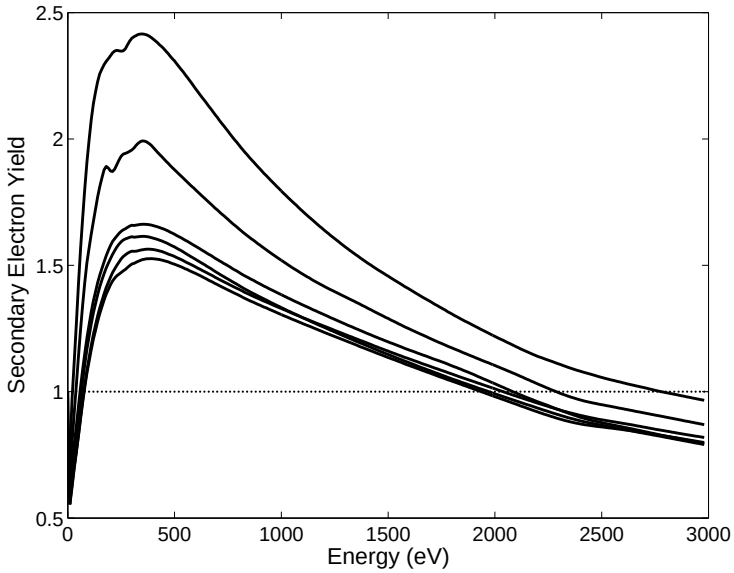

Figure 5. SEY of six TiN/Al samples as received, and measured at normal incidence. δ_{max} for these samples is found in Table 1

The highest yield sample had a high concentration of hydrocarbons (from XPS - Table 1), and some Al as aluminium oxide. Both of these species have elevated SEY.

Table 1
Surface chemical concentrations of TiN/Al samples.

Sample	Ti At%	N At%	Contamination	δ_{max}
#1	24	22	Cl (1%)	1.5264
#2	27	23	-	1.6622
#3	26	24	-	1.6148
#4	5	6	C (50%) - Al (4%)	2.4155
#5	25	22	Mg (2%)	1.5638
#6	18	20	Mg (4%) - C (25%)	1.9922

In most of the samples measured, the XPS amount of C is less than 15% surface atom%, which is a typical value for a clean surface exposed to air.

Samples #4 and #6 are contaminated with hydrocarbon, aluminium oxide and magnesium oxide and therefore the SEY results are not those for clean homogeneous TiN, Table.1.

δ_{max} of the as-received TiN/SS samples, also provided by BNL, varied from 1.7 to 2, when bombarded by a primary beam impinging the surface at 23° from normal incidence, see Fig.6. Again, the thickest samples display the lowest values for the SEY. All of these films were coated in one run, in the same setup, following the procedure described in [9]. The thicknesses of the samples should be identical. Only 3 samples of 6 had similar thicknesses, as shown in Fig.4.

Table 2
Surface chemical concentrations of TiN/SS samples.

Sample	Ti At%	N At%	Contamination	δ_{max}
#b	16	15	Na (2%)	1.7594
#c	20	24	-	1.7694
#d	14	15	-	1.7657
#e	13	13	-	1.9965
#f	14	15	Na (1%)	1.9917

The differences in the SEY, in Fig.6, are surface chemistry and possibly roughness. At energies above 2 keV, electrons penetrate through the ∼150 nm of the TiN film and reach the substrate, suggesting that the bend in the SEY plots

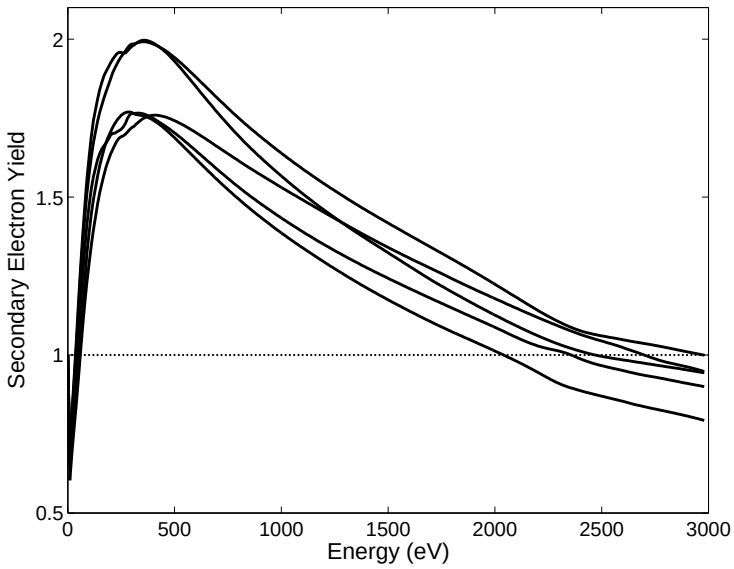

Figure 6. SEY of five TiN/SS samples, as received, measured at 23° primary incidence. δ_{max} for these samples is found in Table 2.

(TiN/Al and TiN/SS) seen at this energy is due to a substrate backscatter effect as shown in Fig.5 and 6. The electron backscattering coefficient increases with the atomic number of the elements.

3.2 Electron conditioning, bake and related evolution of the SEY

Surface conditioning of two TiN films, deposited on Al and SS substrates, with ∼130 eV electrons, was carried out. In the X-band proposal for the ILC (International Linear Collider) positron damping ring, the average energy of electrons from the cloud was computed to be 130 eV [16]. The effect of electron bombardment on the SEY of TiN over an Al and SS substrate is shown in Fig.7. These results are in agreement with data obtained elsewhere at other energies [4,12], and thus within this energy range, there is a weak dependence with the conditioning electron beam energy. The evolution of the TiN SEY during the electron conditioning shows a smoothing of the irregularities observed near δ_{max} as well as a shift of the maximum energy, to lower energy, where the δ_{max} occurs. The bend at high primary energy in the SEY curves disappears as a function of increasing electron dose. This observation is important as it rules out the previous proposed explanation on an extra contribution in the SEY due to backscattered electrons from the substrate.

The SEY evolution might be explained by the removal or dissociation of contaminants at the surface by electron stimulated desorption (ESD). It is possible that, during air exposure, some of the N of the TiN film was displaced by oxygen. Electron bombardment then breaks the TiO_2 into low-SEY defective

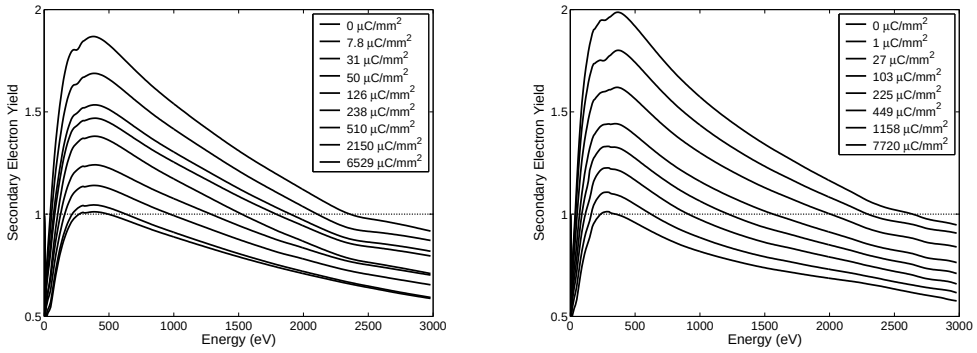

Figure 7. Electron conditioning of TiN/Al #2 (left) and TiN/SS #e (right) sample at 23° primary incidence and 130 eV energy. Values of the SEY are monotonically decreasing from the top curve at 0 μC/mm^2 to bottom curve at 6529 μC/mm^2 or 7720 μC/mm^2. δ_{max} is plotted in Fig.9.

suboxide. Suboxides of many metals are metallic in their electronic structure [4], and clean metals tend to have lower SEY than their oxidized counterparts, for examples see ref.[17]. As a result of electron bombardment, the SEY of our technical TiN becomes similar to that of a freshly deposited TiN film [3].

Two TiN/Al samples provided by Lawrence Berkeley National Laboratory (LBNL) with a deposited thickness of 150 nm were also measured. The samples (#1 and #2) in their as-received state have a δ_{max} of 1.8 to 1.9. No bend can be seen in the SEY plots at 2 keV or more, as shown in Fig.8. TiN was evaporated from a stoichiometric target with an argon plasma of 1.4 mTorr.

The effect of a sample bake of 150°C for 2 hours, then an additional 5 hours on one of the samples, was investigated. The heat treatment reduces the δ_{max} to 1.7 and 1.6 respectively, see Fig.8 top figure. A similar reduction from an as-received TiN sample from CERN was previously obtained [6]. The CERN sample SEY dropped from an initial δ_{max} of 1.6 to a δ_{max} of 1.45. From our test, a 7 hour bake does not much further reduce the SEY than a 2 hour bake. Results of higher temperature treatment can be found in [2] and [6]. The sample was then left in vacuum up to 12 days, bottom figure of Fig.8 (top curve) at a residual pressure of $\sim 5.10^{-10}$ Torr, resulting in gas re-adsorption and a rise in the SEY. The SEY curve of the sample left 12 days in the vacuum is almost identical to the 2 hour bake curve.

Finally, sample #1, after being baked at 150°C and left in vacuum for 12 days, was then exposed to an electron conditioning of energy 130 eV. The reduction of δ_{max}, from 1.7 ("12 days in vac", as shown in Fig.8) to 1.1, obtained with a dose of 5743μC/mm^2 is displayed in Fig.8 and Fig.9 with the following label : TiN/Al#1(LBNL-Baked 150C). The reduction of δ_{max} due to electron conditioning of an as-received sample is also plotted in Fig.9 with the legend TiN/Al#2(LBNL-as received). Electron conditioning is as efficient at lowering the δ_{max} for a TiN film as it is on other technical surfaces.

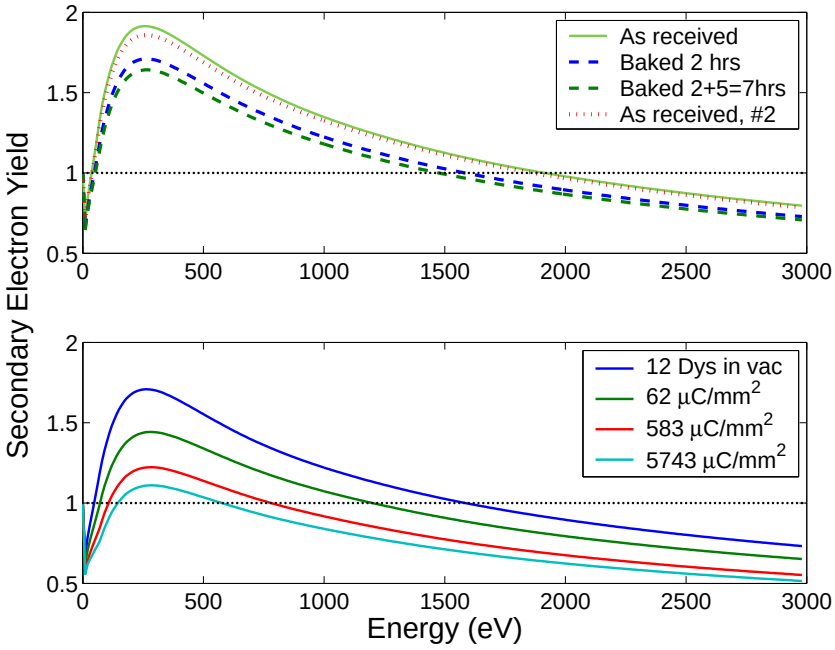

Figure 8. SEY of TiN/Al #1, from LBNL, under different conditions. As-received and baked at 150°C - top figure, SEY is monotonically decreasing. Vacuum recontamination and conditioning by 130 eV electrons - bottom figure, SEY is monotonically decreasing. Measurement performed at 23° primary incidence. TiN/Al #2 as received is also shown.

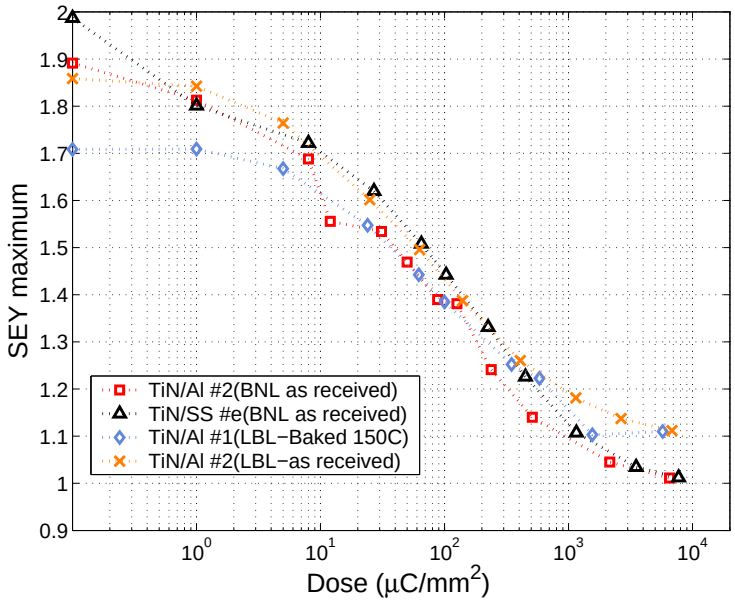

Figure 9. SEY max, measured at 23° primary incidence, during electron conditioning of TiN/Al and TiN/SS

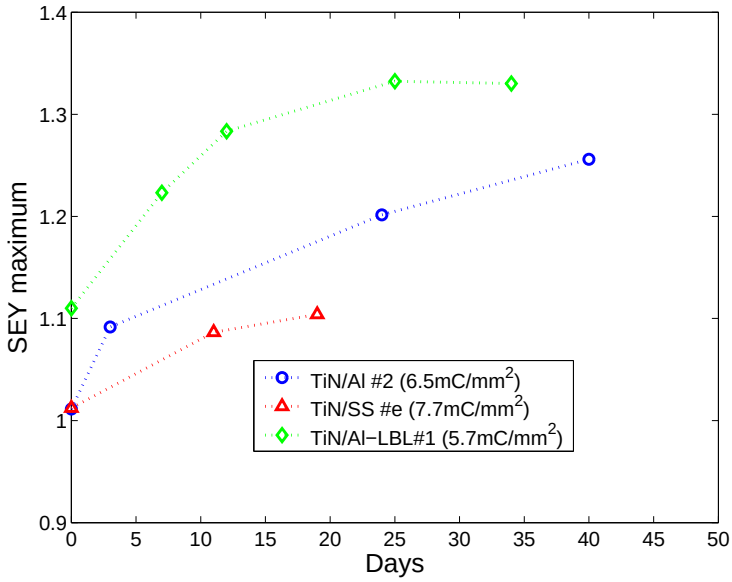

Figure 10. SEY max, measured at 23° primary incidence, during recontamination in a vacuum of a few 10^{-10} Torr

TiN films are fairly chemically passive, but leaving them in vacuum after they have been exposed to electron bombardment leads to some recontamination, presumably because of defect formation (new adsorption sites) [18]. As a result of recontamination, the SEY increases with exposure time as plotted in Fig.10 for three different samples. Intermittently during this period, samples were transferred from the load lock chamber at a pressure of $\sim 10^{-8}$ Torr to the measurement chamber at a pressure in the mid 10^{-10} Torr scale. The exposure to an unbaked load lock chamber vacuum, for a short period of time, seems not to affect the monotonic evolution of the SEY, as shown in Fig.10.

3.3 Application of TiN coating on an artificially rough surface

In some location such as the damping rings of the ILC, the as-installed SEY of the TiN coating will not be acceptable for operation [1]. It is known that roughness can decrease the SEY, so applying the TiN coating to an artificially roughened aluminium surface, like the sample pictured in Fig.11, provides a way of lowering the initial SEY of a non-conditioned surface.

For this test, a surface with a pattern of triangular grooves was fabricated. The triangular groove parameters are 1 mm depth and an opening angle, α, of 40°. Theoretical estimations of the reduction, for triangular and rectangular patterns, of the SEY can be found in [19,20]. Results of the improvements on the SEY obtained by the roughness and the coating of the sample is presented in Fig.12. As we can see in Fig.12, δ_{max} from the uncoated flat aluminium decreases from 3.2 to 2.4 on the uncoated grooved part. An additional reduction

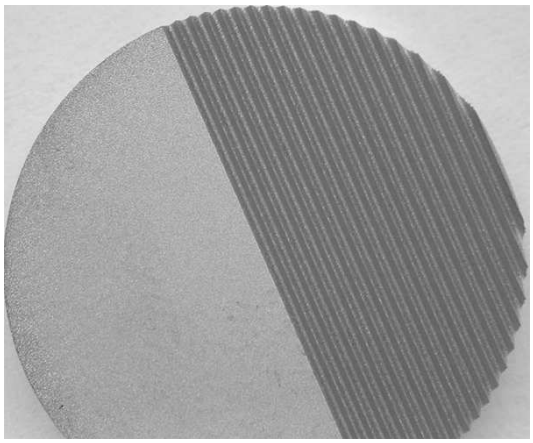

Figure 11. Al 6063 alloy sample half flat and half grooved. Triangular grooves are 1 mm deep and full opening angle, α, is 40°

is achieved by coating the grooved part versus the uncoated, see Fig.12 solid lines.

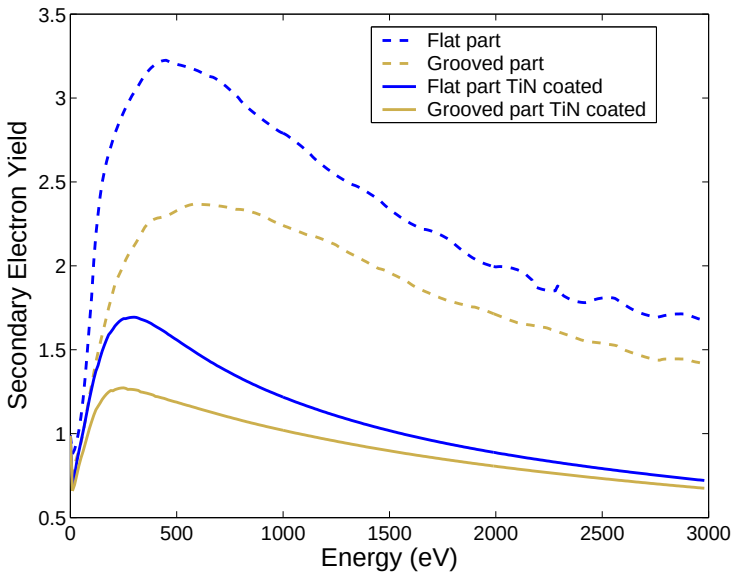

Figure 12. SEY comparison, at normal primary incidence, of a bare Al 6063 sample artificially triangular grooved, then coated by TiN

4 Results and Comments for the NEG thin films

4.1 SEY results from TiZrV NEG film

An alternative SEY-reducing coating to TiN is sputter-deposited TiZrV getter. Two samples were tested, one TiZrV/SS of $\sim 2\mu$m thickness provided by

CERN and one TiZrV/Al of $\sim 1\mu$m thickness from SAES® Getters. NEG, when activated, shows a drastic reduction of its SEY, as shown in Fig.13 and refs. [7,16]. The initial δ_{max}, "as received", is 2 and decreased upon activation to 1.3.

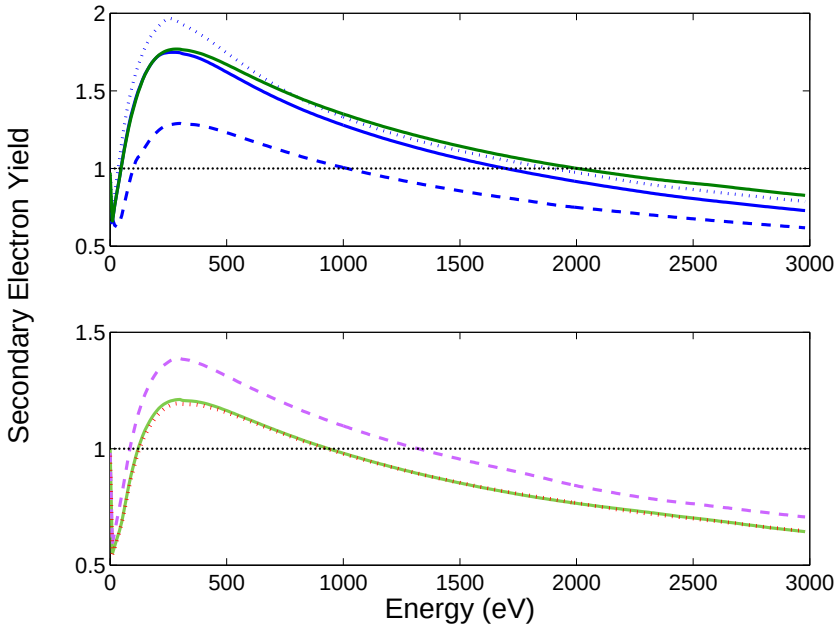

Figure 13. SEY of TiZrV/SS. Top figure : as received (dotted line), activated at 210°C, 2 hrs (dashed line, lower SEY max) and vacuum recontaminated after 134 days at normal incidence and 145 days at 23° incidence (solid line). Bottom figure: electron conditioning (solid line) vacuum recontaminated after 34 days (dashed line) and re-activated, 210°C, 2 hrs (dotted line)

It is also interesting to follow the behaviour of the SEY curves when the sample is exposed to a residual gas background in the high 10^{-10} Torr scale for an extended period of time. The SEY of the TiZrV/SS goes up with time when exposed to even such good vacuum, reaching 1.75 after 145 days, see Fig.13 and Fig.14, open circles. Using the average pressure of 10^{-9} Torr in the system for the 145 days the NEG was in vacuum, we compute an N_2 equivalent exposure of 12528 L (1 L= 10^{-6} Torr-s). In ref.[7], it was found that the influence on the SEY after exposure to 30 000 L of CO, CO_2, H_2O and H_2 is rather small. δ_{max} increased from 1.1 (fully activated CERN NEG) to 1.35 (max). Thus according to [7], the SEY of an activated TiZrV coating left under UHV vacuum should not exceed the critical value of 1.35.

Recent results obtained at CERN, from electron cloud (EC) studies for the Large Hadron Collider (LHC) [21], agree with a saturated SEY value below 1.4 [7]. In the CERN-LHC experiment carried out at the Super Proton Synchrotron (SPS), a section of the machine was replaced with a TiZrV NEG-coated chamber. After activation (200°C, 2 hours) the section was opened to an unbaked vacuum from the SPS. After the NEG was saturated and in the

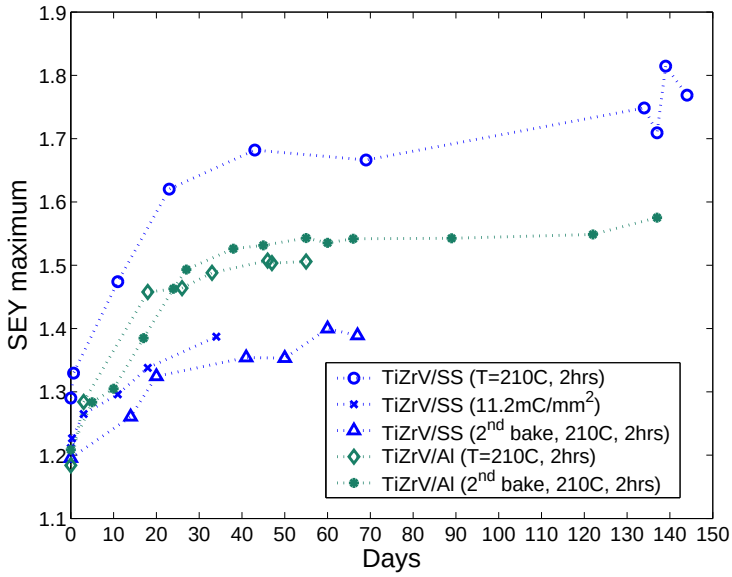

Figure 14. SEY max of the NEG during recontamination in a vacuum of a few 10^{-10} Torr. The TiZrV/SS (open circle) was measured using an electron beam impinging at normal incidence, the others at 23°.

presence of an LHC-type beam, no EC developed, suggesting that the SEY must be below 1.4. This CERN experiment is identical to our experiment, where the sample in the measurement chamber occasionally was exposed to the unbaked vacuum of the load lock, for less than 5 minutes at a time, or was exposed to desorbed gas either from a baked sample or from the gas released during electron conditioning. The discrepancy between our other result (δ_{max} = 1.8), after an initial activation, and the CERN one (δ_{max} = 1.4) is not yet understood and under study.

However, our CERN getter sample was then activated a second time (Fig.13, dotted line). This time the δ_{max} dropped to 1.2. The value of δ_{max} upon re-contamination in UHV went up to 1.4 and appears to have saturated, blue triangles in Fig.14. We note that after electron conditioning and 34 days in a vacuum of a few 10^{-10} Torr, the δ_{max} is ≈1.4 (Fig.14, blue crosses). Thus, these two results are in agreement with CERN data. It is also important to keep in mind that an activated NEG surface will not "remember" its previous surface chemical state. For example the chemical state of a surface which has been conditioned by 130 eV electrons, is "erased" by re-activation.

Results similar to the CERN sample were obtained for the SAES getter sample, i.e TiZrV/Al (δ_{max} = 1.2 after activation), which reached 1.45 after having been left 18 days in vacuum, as shown in Fig.14 (gray diamonds). During the 50 days the sample was in vacuum, the δ_{max} saturated (1.5), or was evolving very slowly. During the time this TiZrV/Al was kept under vacuum, other samples were loaded into the measurement system and a TiN/Al sample was baked. Hence, the TiZrV/Al has seen unbaked vacuum ($\sim 5.10^{-9}$ Torr) and

thermally-desorbed gas from the TiN/Al.

A second bake was then performed on the SAES sample and the evolution of SEY versus time is plotted in Fig.14 (gray asterisk). The average pressure in the system, over time, was below 10^{-9} Torr. The δ_{max} reached 1.54 and appeared to level off. After 137 days that this TiZrV/Al sample was left in vacuum, electron conditioning was performed. Results are plotted in Fig.15 (tilted pale triangle). δ_{max} decreased from 1.57 to 1.07 at a dose of 8425 μC/mm^2, and the maximum energy associated to δ_{max} shifted from 330 eV to 370 eV.

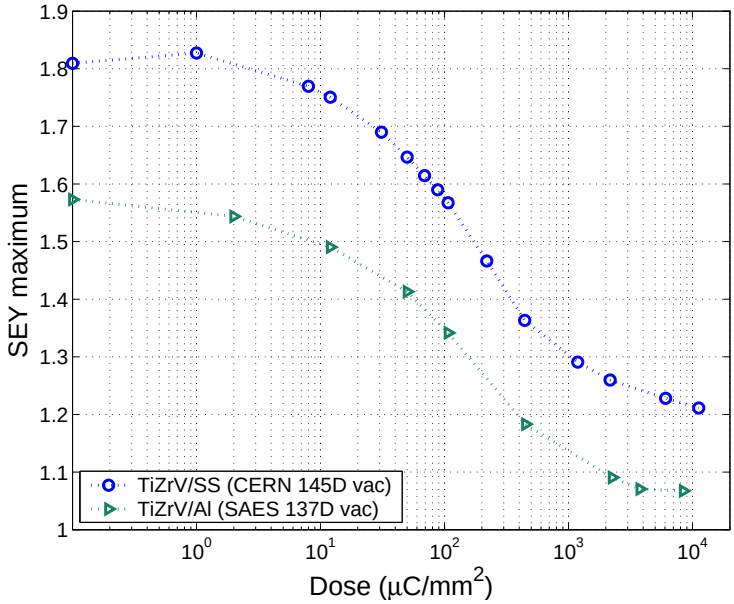

Figure 15. SEY max, measured at 23° primary incidence, during electron conditioning of TiZrV/SS and TiZrV/Al.

These are pertinent results, suggesting that it might be necessary for TiZrV NEG kept in an air environment for a while, to be activated twice to achieve its full properties.

4.2 XPS analysis of the C1s and Ti2p peak

XPS analysis was carried out to observe the evolution of the carbon chemistry from bake through conditioning as well as monitoring the effect of recontamination in UHV. In Fig.16 and Fig.17 are displayed C1s photopeaks obtained by doing XPS at a 0.25 eV step. A few plots were taken with 1 eV step. All XPS spectra were collected at room temperature.

The XPS data obtained for the TiZrV/SS during three different processes is shown in Fig.16. On the left hand side, the NEG is baked at 210°C for 2 hours, then it is left in vacuum. The C1s data shows 3 peaks : 283 eV

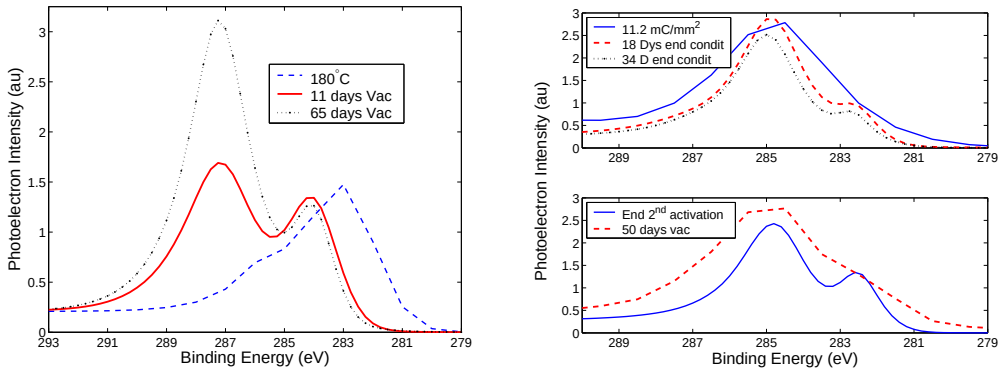

Figure 16. XPS C1s peak, fits, from CERN TiZrV/SS NEG film, after different processes.

285 eV (amorphous/graphite) and 288 eV (oxidized C-O). A C surface will show a single peak at 285 eV, binding energy (BE). A single bonded C-O surface will create a peak at higher BE, 288 eV. During NEG activation a peak at 283 eV appears, as shown on the curve labelled : NEG at 180°C, see Fig.16. This spectrum was taken at the end of the activation, when the NEG was still warm. The 283 eV BE peak is a typical metal carbide state, probably of Ti (Ti-C) which should be present after a fully successful activation [7]. The XPS spectrum of the carbon from the TiZrV/SS, after the two activations, shows the presence of carbide and amorphous/graphite carbon peaks.

After the first activation, see Fig.16 left plots (NEG at 180°C), the carbide at 283 eV BE disappears due to pumping action of the activated NEG. The spectrum shifts to pure C and oxidized C, respectively at 285 eV and 288 eV BE; comparison of curves labelled "NEG at 180C" and "NEG 11 days Vac". After 65 days in vacuum, the oxidized C peak increases. The SEY reflects this change in chemistry, as shown in Fig.13 and 14. After the second activation, right bottom plot in Fig.16, the carbon chemistry is quite different. The carbide peak after 50 days in vacuum is still present. The broadening, results of the 1 eV resolution, of the "50 days in vac" spectrum is due to oxidation of the carbon. This oxidation, however, is minimal and the δ_{max} saturates below 1.4, Fig.14 (blue triangles).

This chemistry scenario, for CERN NEG, is reproduced with the SAES getter TiZrV/Al, in Fig.17 (left and right plots). The fully activated NEG presents a carbide peak (283 eV) and a amorphous/graphite carbon peak (285 eV).

When left in an UHV atmosphere, moderate carbon oxidation occurs and a peak appears at ∼289 eV BE. The NEG pumped the residual gas and the carbon peak (285 eV) rose. Oxygen pumped by the NEG is probably bounded on the Ti and the Zr and not on the C. However, in one case, the carbon did highly oxidize (C=O, double bonded) as plotted in Fig.16 (left) and, as a result, the SEY did not saturate below 1.4, as expected [7].

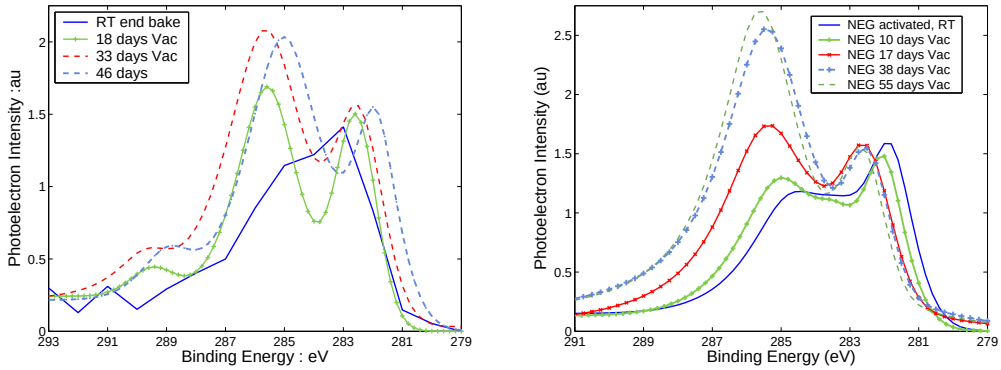

Figure 17. XPS C1s peak, fits, of a TiZrV/Al film after first (left) and second (right) bake out, and left in UHV.

During the processes the getters have endured, we have monitored the evolution of Ti $2p_{1/2}$ and $2p_{3/2}$. No shift in BE energy or peaks intensity was observed. The SEY max of the TiZrV/Al, after one activation, levels off around 1.5, Fig.10 (red diamonds). As a comment, the 283 eV peak is never present on a TiN thin film, either from heating at 150°C or from electron conditioning. Very special conditions can make it appear, for example, by bombarding a TiN film with N_2^+ ion in a 10^{-4} Torr atmosphere of ethylene (C_2H_4) [22].

5 Conclusion and Perspective

The variation in the production of thin TiN film, prepared at the same time in the same system has been presented. This variation is important in an accelerator system where EC can arise. An inhomogeneously coated beam vacuum chamber will have a patchy δ_{max}. For the ILC damping ring, where the onset of the EC is a sudden phenomena, as documented in [1], inhomogeneous coating will create locations where the EC can develop and cause beam blow up and instabilities. However, as the EC develops, conditioning of the surface by electrons will bring the SEY to a value where the EC will be suppressed. The δ_{max} reached at a dose of 1 mC/mm^2 was 1.1 for TiN on SS or Al substrates. Recontamination in UHV does result in an increase of the SEY by less than 20%, as shown in Fig.10. Combining a triangular grooved surface with a TiN coating, which has been exposed to air, is an efficient solution for suppressing the EC, see Fig. 12. However, an artificially rough surface interacts more strongly with a passing beam than does a smooth one, so care has to be taken in the design of such surfaces.

In the case of TiZrV/SS, the influence of activation, electron conditioning and pumping recontamination were investigated. δ_{max} increased from $\sim$1.2, obtained after activation, and seemed to saturate at $\sim$1.4 after 40 days of exposure to a vacuum of $\sim 5.10^{-10}$ Torr. This second set of data after activation

agrees with CERN results [7], i.e. that saturated NEG and conditioned NEG both have a δ_{max} below 1.4. The TiZrV/Al sample produced similar results, i.e. the maximum SEY levelled off at 1.5 after 46 days.

Electron conditioning of TiZrV/Al NEG by 130 eV electron beam, is also efficient at reducing the SEY of the surface below 1.2 at a dose of 1 mC/mm^2. These results are very encouraging for choosing TiZrV as a solution for suppressing the EC. The SEY reached during recontamination by an UHV atmosphere, compared to the SEY obtained by exposure to a high dose of gas (CO_2, CO, H_2O and H_2) is different and is above the 1.35 δ_{max} limit obtained in ref.[7]. Studies on a Mg getter surface show a difference in chemistry between a surface briefly exposed to air or left in air for a longer period of time [23]. A Mg surface briefly exposed to air forms MgO oxide. When left in air for a month, chemistry of the Mg surface shows that the main oxide is $Mg(OH)_2$. Mobility of atoms on the surface might be the reason for the difference between a dose activated NEG surface and a NEG left pumping the residual gas of an UHV system.

In an accelerator, the EC is going to be one of the elements responsible for conditioning the walls of the beam chambers. When the SEY decreases, the efficiency of the electron conditioning will decrease as well (fewer electrons, slower conditioning), reaching a limit where the recontamination from the accelerator vacuum dominates, thence making the EC reappear. However, in a dynamic vacuum, the contribution of photon [24] and ion conditioning could be the key to preventing the re-increase of the SEY. We are measuring the SEY of thin film coatings, exploring durability and conditioning strategies, investigating a new surface profile design and finally planning to install test demonstration chambers in PEP-II at SLAC. In particular, coated samples will be arranged in a high synchrotron radiation region and grooved chambers will be installed in the straight sections in PEP-II. We also plan to investigate ion conditioning by several different species of ions, as well as different impact energies. This study will be based on the expected vacuum conditions and beam parameters of the ILC damping ring.

6 Acknowledgments

We would like to thank P. He and H.C. Hseuh at BNL for providing the TiN samples on aluminium and on stainless steel, V. Rouzinov, S. Faggian and C. Benvenuti from the EST group at CERN for the TiZrV sample. We also thank A. Wolski, D. Lee and K. Kennedy at LBNL for the production of thin film samples of TiN and TiZrV. Most valuable was the work of G. Collet and E. Garwin at SLAC for converting and baking the XPS system for use on SEY measurements.

References

[1] M. Pivi et al. Recent Electron-Cloud Simulation Results for the Main Damping Rings of the NLC and the TESLA Linear Colliders. In *PAC, Portland, Or, USA*, 2003. SLAC-PUB-9814.

[2] A.R. Nyaiesh et al. Properties of thin antimultipactor TiN and Cr_2O_3 coatings for klystron windows. *Journal of Vacuum Science and Technology*, A4(5), 1986.

[3] P. Prieto and R.E. Kirby. X-ray photoelectron spectroscopy study of the diference between reactively evaporated and direct sputter-deposited TiN films and their oxidation prperties. *Journal of Vacuum Science and Technology*, A13(6), 1995.

[4] R.E. Kirby F.K. King. Secondary Emission Yield from PEP-II accelerator material. *Nuclear Instruments and Methods in Physics Research A*, A469, 2001.

[5] B. Henrist, N. Hilleret, C. Scheuerlein, M. Taborelli. The secondary electron yield of TiZr and TiZrV non-evaporable getter thin film coatings. *Applied Surface Science*, 172:95–102, 2001.

[6] N. Hilleret et al. The Secondary Electron Yield of Technical Materials and its Variation with Surface Treatments. In *EPAC , Vienna, Austria*, 2000.

[7] C. Scheuerlein. The Activation of Non-evaporable Getters Monitored by AES, XPS, SSIMS and Secondary Electron Yield Measurements. Technical report, CERN- THESIS- 2002- 026, 2002.

[8] R.E. Davies and J.R. Dennison. Evolution of Secondary Electron Emission Characteristics of Spacecraft Surfaces. *J.Spacecraft*, 34 (4):571, 1997.

[9] P. He et al. Development of TiN coating for SNS Ring Vacuum Chambers. In *PAC 2001*, 2001.

[10] S. Kato, M. Nishiwaki. Study on Electron Emission from Some Metals and Carbon Materials and the Surface Characterization. In *49th AVS*, 2002.

[11] S. I. Castañeda et al. Effects of air exposure on ion beam assisted TiN:O coatings to prevent multipactor. *Journal of Vacuum Science and Technology*, A21(6), 2003.

[12] L. Galán, et al. Surface Treatment and Coating for the Reduction of Multipactor and Passive Intermodulation (PIM) Effects in RF Components. In 4^{th} *International Workshop on Multipactor, Corona and PIM in Space Hardware*, 2003.

[13] F. Le Pimpec, F. King, R.E. Kirby, M. Pivi. Secondary Electron Yield Measurements of TiN Coating and TiZrV Getter Film. Technical report, SLAC TN03-052, 2003.

[14] J.C Vickerman, editor. *Surface Analysis : The Principal Techniques.* J. Wiley & Sons, 1997.

[15] K.M. Welch. Low Pressure Crossed Field Vacuum Sputtering of Thin Films for Multipactor Suppression Using a Simple Diode Array. Technical report, SLAC-Pub-1472, 1974.

[16] F. Le Pimpec, F. King, R.E. Kirby, M. Pivi, G.Rumolo. The Continuing Story of Secondary Electron Yield Measurements from TiN Coating and TiZrV Getter Film. Technical report, SLAC TN04-046, 2004.

[17] David R. Lide, editor. *Handbook of Chemistry and Physics.* 74^{th} edition. CRC PRESS, 1994.

[18] J.N. Wilson et al. Carbon coupling on titanium oxide with surface defects. 562:L231, 2004.

[19] A.A. Krasnov. Molecular pumping properties of the LHC arc beam pipe and effective secondary electron emission from Cu surface with artificial roughness. *Vacuum*, 73:195, 2004.

[20] G. Stupakov and M. Pivi. Suppression of the Effective Secondary Electron Emission Yield for a Grooved Metal Surface. In *Electron Cloud Workshop, Napa valley USA*, 2004. http://icfa-ecloud04.web.cern.ch/icfa-ecloud04/agenda.html.

[21] A. Rossi. SEY and electron cloud build-up with NEG materials. In *Electron Cloud Workshop, Napa valley USA*, 2004. http://icfa-ecloud04.web.cern.ch/icfa-ecloud04/agenda.html.

[22] I. Nakamura et al. Surface Modification of TiN Films by Nitrogen Ion Beam Irradiation in Ethylene Gas Atmosphere. *Vacuum*, 74:659, 2004.

[23] K. Asami and S. Ono. Quantitative X-Ray Photoelectron Spectroscopy Characterization of Magnesium Oxidized in Air. *Journal of the Electrochemical Society*, 147 (4):1408, 2000.

[24] V. Baglin et al. Measurements at EPA of Vacuum and Electron-Cloud Related Effects. In *Chamonix 2001, LEP performance*, 2001.

List of Figures